CHEMISTRY OF MATERIALS

ARTICLE

pubs.acs.org/cm

Novel Starburst Triarylamine-Containing Electroactive Aramids with Highly Stable Electrochromism in Near-Infrared and Visible Light Regions

Hung-Ju Yen, Hung-Yi Lin, and Guey-Sheng Liou*

Functional Polymeric Materials Laboratory, Institute of Polymer Science and Engineering, National Taiwan University, 1 Roosevelt Road, fourth Sec., Taipei 10617, Taiwan

Supporting Information

ABSTRACT: A series of solution-processable near-infrared (NIR) electrochromic aromatic polyamides with starburst triarylamine units in the backbone were prepared by the phosphorylation polyamidation from a newly synthesized diamine monomer, *N*,*N*-bis[4-(4-methoxyphenyl-4′-aminophenylamino)phenyl]-*N*′,*N*′-di(4-methoxyphenyl)-*p*-phenylenediamine, and two aromatic dicarboxylic acids. These polymers were highly soluble in many organic solvents and showed useful levels of thermal stability associated with high glass-transition temperatures and high char yields (higher than 66% at 800 °C in nitrogen). The polymer films showed reversible electrochemical oxidation and electrochromism with high contrast ratio both in the visible range and NIR region, which also exhibited high coloration efficiency (CE), low switching time, and relatively high stability for long-term electrochromic operation. At the first oxidation stage, the polyamide **Ia** thin film revealed high coloration efficiency in NIR (CE = 290 cm^2/C) region with reversible electroactive stability (more than 10000 times within 0.6% loss relative to its initial injected charge). As the dication radical form of second oxidation stage, the polymer film still exhibited excellent electrochromic/electroactive stability (more than 10 000 cyclic switches) with enhanced CE of 339 cm^2/C.

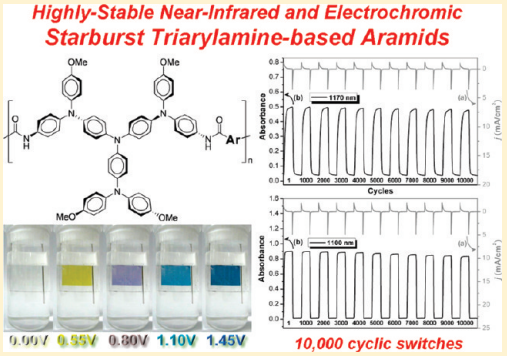

KEYWORDS: polymeric materials, electronic materials, electrochemistry

INTRODUCTION

Electrochromic materials exhibit a reversible optical change in absorption or transmittance upon electrochemically oxidized or reduced, such as transition-metal oxides, inorganic coordination complexes, conjugated polymers, and organic molecules.[1] Despite the fact that the electrochromic devices were mostly based on inorganic oxides, nevertheless, the organic material has several advantages over the former ones, such as processability, high coloration efficiency, fast switching ability, and multiple colors within the same material. Initially, investigation of electrochromic materials has been directed toward optical changes in the visible region (e.g., 400−800 nm), proved useful and variable applications such as E-paper, optical switching devices, smart window, and camouflage materials.[2] Increasingly, attention of the optical changes has been focused extending from the near-infrared (NIR; e.g., 800−2000 nm) range to the microwave region of the spectrum, which could be exploitable for optical communication, data storage, and thermal control (heat gain or loss) in buildings and spacecrafts.[3] In recent years, NIR electrochromic materials including transition metal oxides WO_3, organic metal complex (ruthenium dendrimer), and quinone-containing organic materials have been investigated.[4] Wang and Wan[4c−g] made efforts on the quinone-containing electrochromic materials, which revealed high absorption in the NIR upon electrochemical reduction. Reynold[1i,5a] reported color-to-transmissive NIR electrochromic conjugated polymers, their devices exhibited multicolor in neutral state and trasmissive in the oxidized state. In addition to conjugated polymers,[5] *p*-phenylenediamine-containing molecule is an interesting anodic electrochromic system for NIR applications due to its particular intramolecular electron transfer in the oxidized states.

Intramolecular electron transfer (ET) processes were studied extensively in the mixed-valence (MV) systems,[6] and usually employed one-dimensional MV compounds contain two or more redox states. According to Robin and Day,[7] the *p*-phenylenediamine cation radical has been reported as a symmetrical delocalized class III structure with a strong electronic coupling (the electron is delocalized over the two or more redox centers), leading an intervalence charge transfer (IV-CT) absorption band in the NIR region.[8]

In order to be useful for electrochromic applications, some key issues such as long-term stability, multiple colors within the same material, rapid redox switching, high coloration efficiency (CE), and high optical transmittance change ($\Delta\%T$) during operation are indispensable and are playing important roles. Therefore, to achieve a good combination of the above-mentioned parameters is a crucial and ongoing issue. Reynolds' group[5e] studied

Received: December 14, 2010
Revised: March 1, 2011
Published: March 15, 2011

Scheme 1. Synthetic Route to 9Ph4OMe-diamine Monomer 2

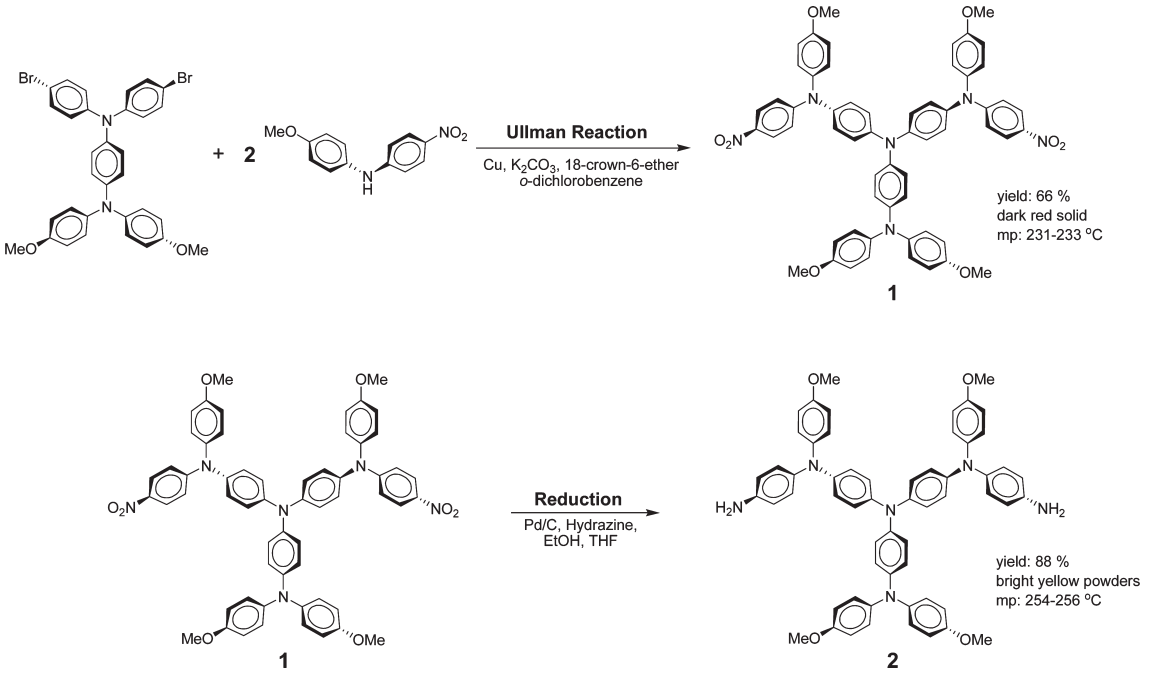

poly(3,4-alkylenedioxy thiophene) films and found that their electrochromic devices retained 90% after 180,000 switching cycles with a high contrast ratio of 75%. The EDOT derivative reported by Wudl's group[5b,c] exhibited high CE and stability after 5000 switching cycles but only with a contrast ratio of 57%. Since 2005, our group has reported several triphenylamine containing electrochromic polymers with interesting color transitions[9] that showed good electrochromic reversibility in the visible region and NIR range. However, most of the polymers could only reveal less than two stages of electrochromism because of the difficulty and complexity in increasing electroactive nitrogen atoms within triarylamine-containing structures. Therefore, our strategy is to design and synthesize the NIR electrochromic starburst triarylamine-based materials with the incorporation of electron-donating substituents at the para-position of phenyl groups, thus could greatly prevent the coupling reactions by affording stable cationic radicals and lowering the oxidation potentials.[10] The advantage of more electroactive sites and better processability than the conventional linear polymer was due to the introduction of starburst triarylamine derivatives into polymer system. The resultant electroactive polymers with high molecular weights and excellent thermal stability should be readily obtained by using conventional polycondensation. Because of the incorporation of packing-disruptive starburst triarylamine units into the polymer backbone, these novel polymers should also show excellent solubility in various polar organic solvents, thus transparent and flexible polymer thin films could be prepared easily by solution casting and spin-coating techniques. This is beneficial for their fabrication of large-area, thin-film electrochromic devices.

In this contribution, we therefore synthesized the diamine monomer, *N*,*N*-bis[4-(4-methoxyphenyl-4′-aminophenylamino)phenyl]-*N*′,*N*′-di(4-methoxyphenyl)-*p*-phenylenediamine (**2**), and their corresponding aromatic polyamides containing starburst triarylamine units with *para*-substituted methoxy groups. The incorporation of electron-donating methoxy substituents is expected to reduce the oxidation potential associated with enhanced electrochemical and electrochromic stability of the result polyamides. Thus, we anticipate that these novel polyamides should be excellent in many aspects such as electrochemical stability with multiple electrochromic switchings, optical response times, coloration efficiency, and high optical contrast in both NIR and visible-light regions.

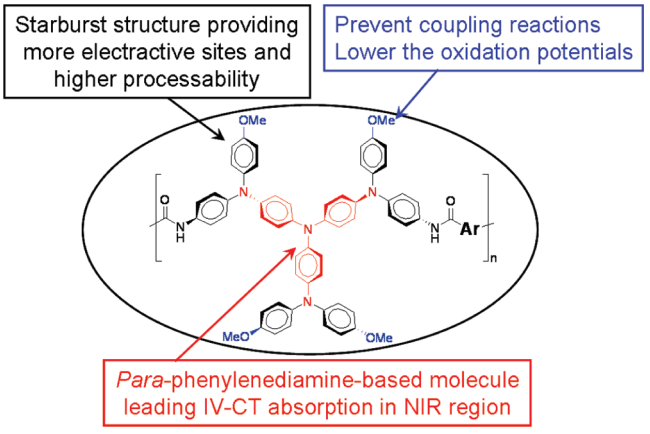

RESULTS AND DISCUSSION

Monomer and Polymer Synthesis. The new starburst diamine monomer **2** was synthesized by hydrazine Pd/C-catalyzed reduction of the dinitro compound **1** derived from *N*,*N*-bis(4-bromophenyl)-*N*′,*N*′-di(4-methoxyphenyl)-*p*-phenylenediamine and 4-methoxy-4′-nitrodiphenylamine by Ullman reaction (Scheme 1). Elemental analysis, FT-IR, and NMR spectroscopy were used to identify structures of the intermediate dinitro compound **1** and the target diamine monomer **2**. The FT-IR

dx.doi.org/10.1021/cm103552k |*Chem. Mater.* 2011, 23, 1874–1882

Scheme 2. Synthesis of Aromatic Polyamides I; Photograph Shows Appearance of the Flexible Films (thickness ≈ 60μm)

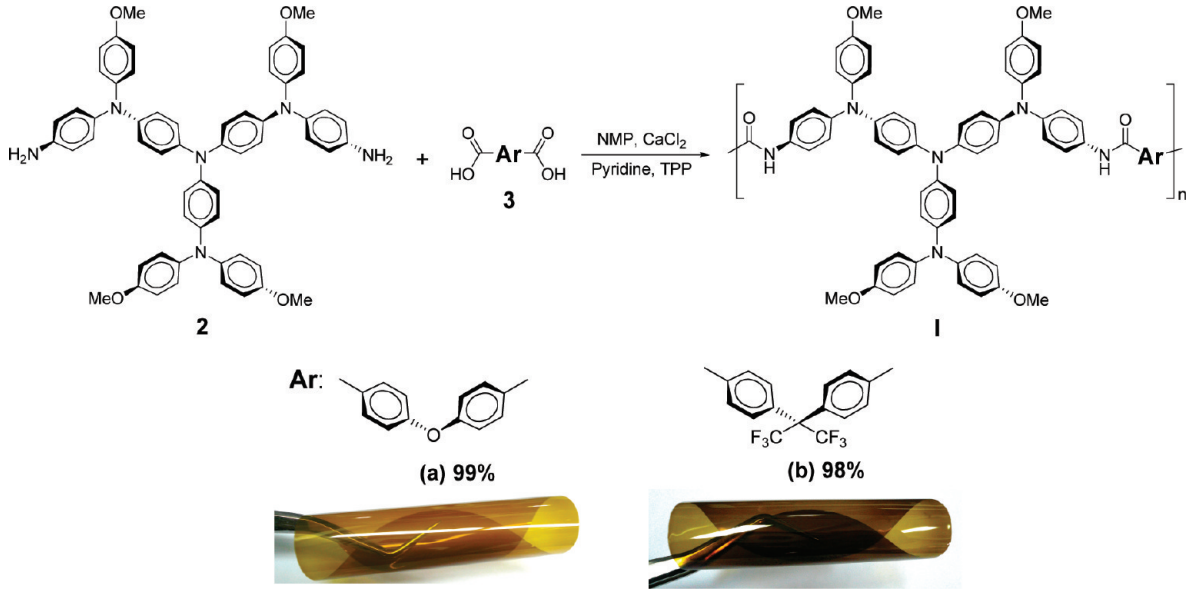

spectra of these two synthesized compounds are illustrated in Figure S1 in the Supporting Information. The nitro groups of compound **1** showed characteristic bands at around 1587 and 1311 cm^{-1} due to NO_2 asymmetric and symmetric stretching. After reduction to diamine monomer **2**, the characteristic absorption bands of the nitro group disappeared and the primary amino group revealed the typical absorption pair at 3446 and 3365 cm^{-1} (N−H stretching). The ^1H NMR and ^{13}C NMR spectra of the intermediate dinitro compound **1** and diamine monomer **2** are illustrated in Supporting Information (Figure S2−S4) and agree well with the proposed molecular structures. Thus, the results of all the spectroscopic and elemental analyses suggest the successful preparation of the target diamine monomer.

According to the phosphorylation technique described by Yamazaki,[11] these novel polyamides **I** with starburst arylamine moieties were synthesized from the diamine monomer **2** and two aromatic dicarboxylic acids **3** (Scheme 2). The polymerization was carried out via solution polycondensation using triphenyl phosphite and pyridine as condensing agents. All polymerization reactions proceeded homogenously and gave high molecular weights. The obtained polyamides had inherent viscosities in the range of 0.27−0.36 dL/g with weight-average molecular weights (M_w) and polydispersity (PDI) of 69 800−131 000 Da and 1.85−2.13, respectively, relative to polystyrene standards (see Table S1 in the Supporting Information). All the polymers with high molecular weights could afford transparent and tough films via solution casting. The structures of the polyamides were confirmed by elemental analysis, NMR, and IR spectroscopy. The ^1H NMR spectra of the polyamide **Ia** and **Ib** were illustrated in Figure S5 in the Supporting Information and agree well with the proposed molecular structures. As shown in Figure S6 in the Supporting Information, a typical IR spectrum for polyamides exhibited characteristic absorption bands of the amide group at around 3307 (N−H stretch) and 1669 cm^{-1} (amide carbonyl).

Solubility and Film Property. The solubility properties of polymers **I** were investigated qualitatively at 5% w/v concentration and the results are also listed in Table S2 in the Supporting Information. These polyamides were highly soluble not only in polar aprotic organic solvents such as *N*-methyl-2-pyrrolidinone (NMP), *N*,*N*-dimethylacetamide (DMAc), *N*,*N*-dimethylformamide (DMF), dimethyl sulfoxide (DMSO) but also in less polar solvents such as tetrahydrofuran (THF) and $CHCl_3$. Thus, the excellent solubility makes these polymers as potential candidates for practical applications by spin-coating or inkjet-printing processes to afford high performance thin films for optoelectronic devices. As mentioned above, the polyamides **I** could be solution cast into flexible, transparent, and tough films. The appearance and quality of these films are also shown in Scheme 2. Their high solubility and amorphous properties can be attributed to the incorporation of bulky, three-dimensional starburst triarylamine moiety along the polymer backbone, which results in a high steric hindrance for close packing, and thus reduces their crystallization tendency.

Thermal Properties. The thermal properties of polyamides were examined by TGA and DSC, and the thermal behavior data are summarized in Table S2 in the Supporting Information. Typical TGA and DSC curves of polyamides **Ia** and **Ib** in both air and nitrogen atmospheres are shown in Figure S7 in the Supporting Information. All the prepared polyamides exhibited good thermal stability with insignificant weight loss up to 400 °C in nitrogen or air atmosphere even with the introduction of methoxy groups. The 10% weight loss temperatures of these polymers in nitrogen and air were recorded in the range of 480−510 and 495−510 °C, respectively. The carbonized residue (char yield) of these polymers in a nitrogen atmosphere was more than 66% at 800 °C. The high char yields of these polymers can be ascribed to their high aromatic content. The glass-transition temperatures (T_g) of polyamides **I** could be easily measured in the DSC thermograms; they were observed in the range of 224−270 °C, depending upon the stiffness of the polymer chain. The lower T_g value of **Ia** can be explained in terms of the flexible ether linkage in its diacid component.

Electrochemical Properties. The electrochemical properties of compounds **1**, **2**, and the polyamides were investigated by cyclic voltammetry (CV). The compounds were dissolved in anhydrous dichloromethane (CH_2Cl_2) solution (Conc.: 1×10^{-4} mol/L), and the polymers were conducted by cast film

dx.doi.org/10.1021/cm103552k |*Chem. Mater.* 2011, 23, 1874–1882

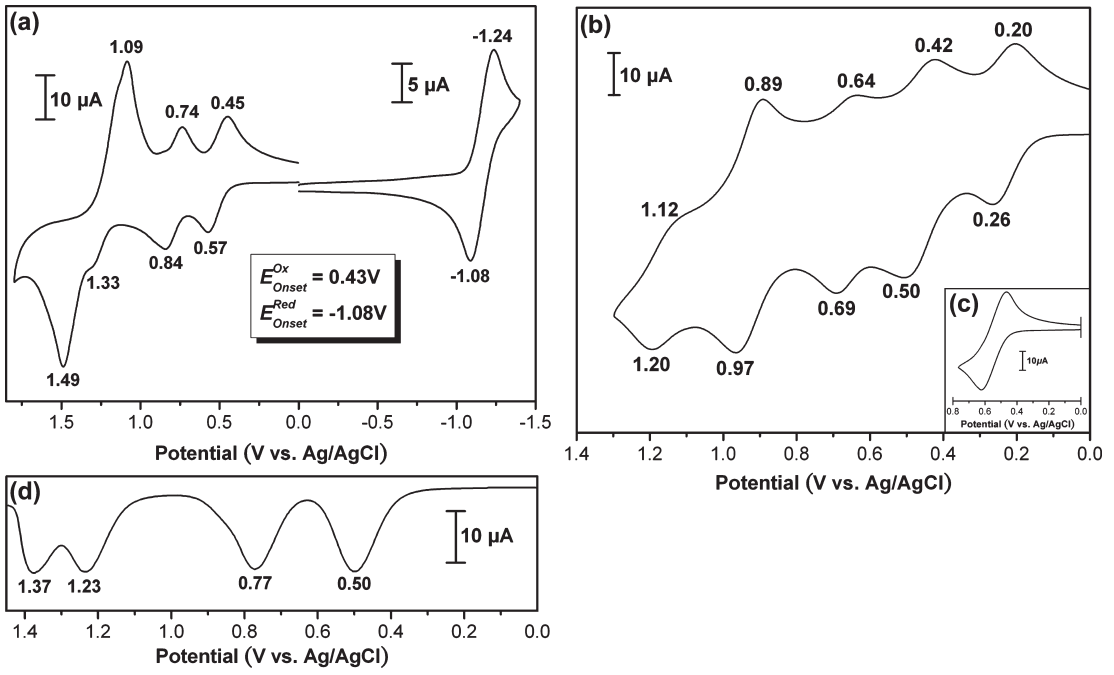

Figure 1. Cyclic voltammograms of (a) 1×10^{-4} M dinitro compound **1**, (b) 1×10^{-4} M diamino compound **2**, (c) ferrocene in CH_2Cl_2 solution containing 0.2 M TBAP at scan rate of 50 mV/s, and (d) differential pulse voltammograms of 1×10^{-4} M dinitro compound **1** in CH_2Cl_2 solution containing 0.2 M TBAP. Scan rate, 5 mV/s; pulse amplitude, 50 mV; pulse width, 50 ms; pulse period, 0.2 s.

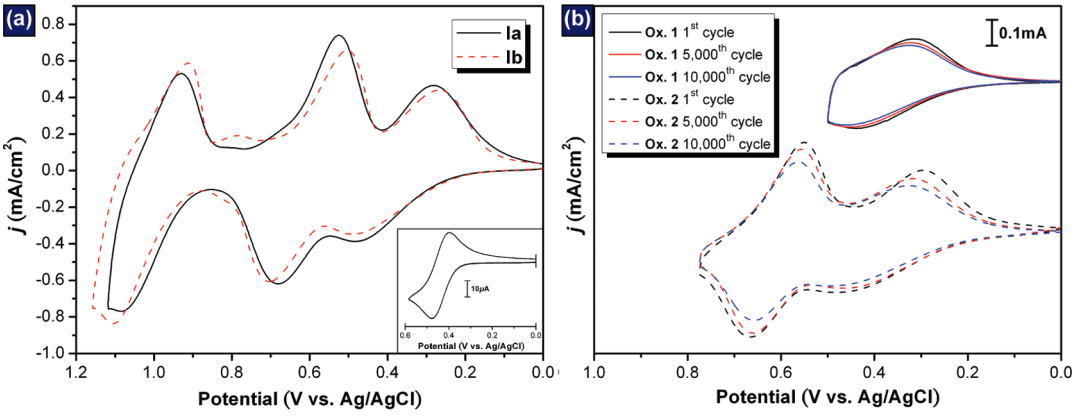

Figure 2. (a) Cyclic voltammetric diagrams of polyamide **Ia** and **Ib** films on an ITO-coated glass substrate and ferrocene (inset) in 0.1 M TBAP/CH_3CN at a scan rate of 50 mV/s. (b) Cyclic voltammograms of polyamide **Ia** on an ITO-coated glass substrate over cyclic scans in CH_3CN solution containing 0.1 M TBAP at scan rate of 25 mV/s.

on an indium−tin oxide (ITO)-coated glass slide as working electrode in anhydrous acetonitrile (CH_3CN), using 0.1 M of tetrabutylammonium perchlorate (TBAP) as a supporting electrolyte in a nitrogen atmosphere. The typical CV diagrams for compounds **1** and **2** are shown in Figure 1. There are four reversible oxidation and one reduction redox couples for compound **1**, and five reversible oxidation redox couples for compound **2**, respectively. As the substituent varies from electron-withdrawing nitro group to electron-donating amino group, the oxidation potential of amino compound **2** was lower than that of compound **1**, indicating the electronic effect of the substituent on the oxidation reaction. In the case of polymer system as shown in the Figure 2 and Figure S8 in the Supporting Information, the CV of polyamides **I** reveal three reversible and one irreversible oxidation processes. During the electrochemical oxidation of the polyamide thin films, the color of polymer film changed from colorless to yellow, purple, bluish green and then to deep blue. Because of the high electrochemical stability and good adhesion between the polyamide thin film and ITO substrate, polyamide **Ia** exhibited reversible CV behavior by continuous 10 000 cyclic scans both in the first and second oxidation stages. The redox potentials of the polyamides as well as their respective highest occupied molecular orbital (HOMO) and lowest unoccupied molecular orbital (LUMO) (versus vacuum) are calculated and summarized in Table 1. The HOMO level or called ionization potentials (versus vacuum) of polyamides **I** could be estimated from the onset of their oxidation in CV experiments as 4.67−4.68 eV (on the basis that ferrocene/ferrocenium is 4.8 eV below the vacuum level with E_{onset} = 0.36 V).

dx.doi.org/10.1021/cm103552k |*Chem. Mater.* 2011, 23, 1874–1882

Table 1. Redox Potentials and Energy Levels of Polyamides

	thin films (nm)		oxidation potential (V)[a]							
polymer	λ_{max}	λ_{onset}	E_{onset}	$E_{1/2(ox1)}$	$E_{1/2(ox2)}$	$E_{1/2(ox3)}$	λ_{max}	E_g (eV)[b] λ_{onset}	HOMO (eV)[c]	LUMO (eV) E_{onset}
Ia	349	410	0.24	0.39	0.61	1.01	1.34	3.02	4.68	1.66
Ib	345	412	0.23	0.39	0.59	1.01	1.27	3.01	4.67	1.66

[a] From cyclic votammograms vs Ag/AgCl in CH_3CN. $E_{1/2}$: average potential of the redox couple peaks. E_p: peak potential of the irreversible fourth oxidation steps. [b] The data were calculated from polymer films by the equation: $E_g = 1240/\lambda_{onset}$ (energy gap between HOMO and LUMO). [c] The HOMO energy levels were calculated from cyclic voltammetry and were referenced to ferrocene (4.8 eV ; onset = 0.36 V).

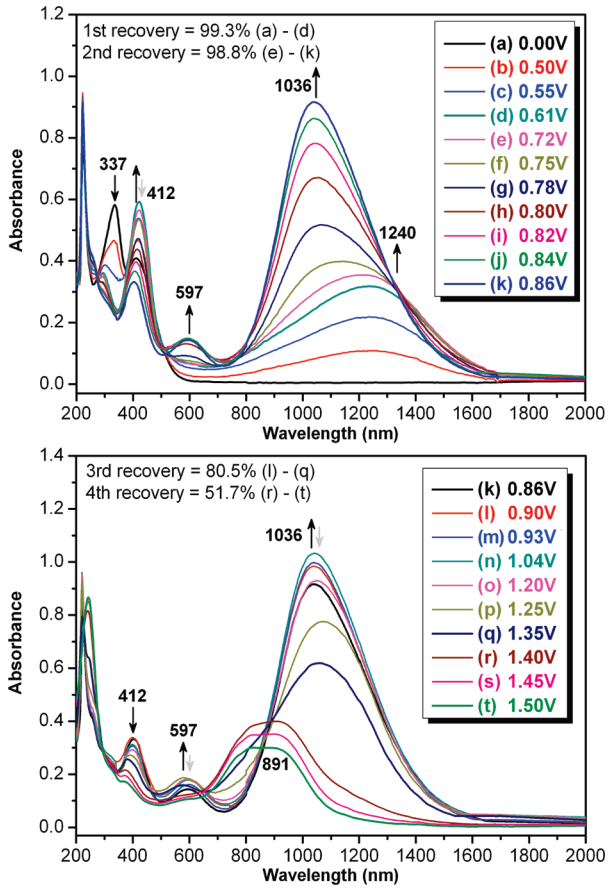

Figure 3. Absorption spectral change of 1×10^{-4} M dinitro compound **1** in CH_2Cl_2 solution containing 0.2 M TBAP at various applied potentials between 0.0 and 1.50 (V vs Ag/AgCl).

Spectroelectrochemistry. Spectroelectrochemical experiments were used to evaluate the optical properties of the electrochromic films. For the investigations, compound **1** and polyamide film were prepared in the same manner as described above, and a homemade electrochemical cell was built from a commercial ultraviolet (UV)−visible cuvette. The cell was placed in the optical path of the sample light beam in a UV−vis−NIR spectrophotometer, which allowed us to acquire electronic absorption spectra under potential control. UV−vis−NIR absorbance curves correlated to electrode potentials of compound **1** is presented in Figure 3. The absorption peaks at 337 and 412 nm are characteristic for compound **1**. After one-electron oxidation (0.00−0.61 V), the original peaks decreased and a broad band at around 1240 nm increased gradually. The first oxidation reversibility was 99% based on the absorbance at 337 nm.[12] When the potential was adjusted to more positive values (0.61−0.86 V) corresponding to the second electron oxidation, the characteristic new peaks at 597 and 1036 nm appeared and the second oxidation reversibility was 99%. For the third oxidative state (0.86−1.35 V), the peak at 1036 nm decreased slightly with a reversibility of 81%. It shows the first, second, and third oxidative states are reversible and highly stable. When the applied potential was adding to 1.50 V, the characteristic peaks new bands at 891 nm appeared, but only 52% absorbance remained implying that the oxidation product (tetracation) was not stable. The same experiment for polyamide **Ia** film exhibited the first, second, third, and fourth oxidation reversibility up to 100, 99, 83, and 59%, respectively.

The typical spectroelectrochemical spectra and three-dimensional % transmittance-wavelength-applied potential correlations of polyamide **Ia** film is presented in Figure 4. In the neutral form (0 V), the film exhibited strong absorption at around 346 nm, characteristic for triarylamine, but it was almost transparent in the visible region. Upon oxidation (increasing applied voltage from 0 to 0.55 V), the intensity of the absorption peak at 346 nm gradually decreased while a new peak at 447 nm and a broad IV-CT band centered around 1170 nm in the NIR region gradually increased in intensity. We attribute the spectral change in visible-light range to the formation of a stable monocation radical $\mathbf{Ia}^{1+}$ in the TPA center of starburst triarylamine moiety. Furthermore, the broad absorption in NIR region was the characteristic result due to IV-CT excitation between states in which the positive charge is centered at different nitrogen atoms, which was consistent with the phenomenon classified by Robin and Day.[6] As the more anodic potential to 0.80 V corresponding to $\mathbf{Ia}^{2+}$, the absorption bands (346 and 447 nm) decreased gradually with new broad bands centered at around 583 and 1100 nm. By further applying positive potential value up to 1.10 V corresponding to $\mathbf{Ia}^{3+}$, the characteristic absorbance at 643 and 824 nm appeared, and the strong IV-CT band at 1079 nm in the NIR region still could be observed. When the applied potential was added to 1.45 V, the absorption bands at 1079 nm decreased gradually with a new broad band centered at around 729 nm. The disappearance of NIR absorption band can be attributable to the further oxidation of $\mathbf{Ia}^{3+}$ species to the formation of $\mathbf{Ia}^{4+}$ in the starburst triarylamine segments. The observed UV−vis-NIR absorption changes in the polyamide **Ia** film at various potentials are reversible and associated with strong color changes. The other polyamide **Ib** showed similar spectral change to that of **Ia**. From the figure shown in Figure 4, the polyamide **Ia** film switches from a transmissive neutral state (colorless; Y: 90; *x*, 0.313; *y*, 0.331) to the first-oxidized state (yellow; Y: 50; *x*, 0.398; *y*, 0.461), second-oxidized state (purple; Y: 21; *x*, 0.278; *y*, 0.271), third-oxidized state (bluish-green; Y: 20; *x*, 0.252; *y*, 0.315), and a fully oxidized state (deep blue; Y; 7; *x*, 0.208; *y*, 0.229). The film colorations are distributed homogeneously across the polymer film

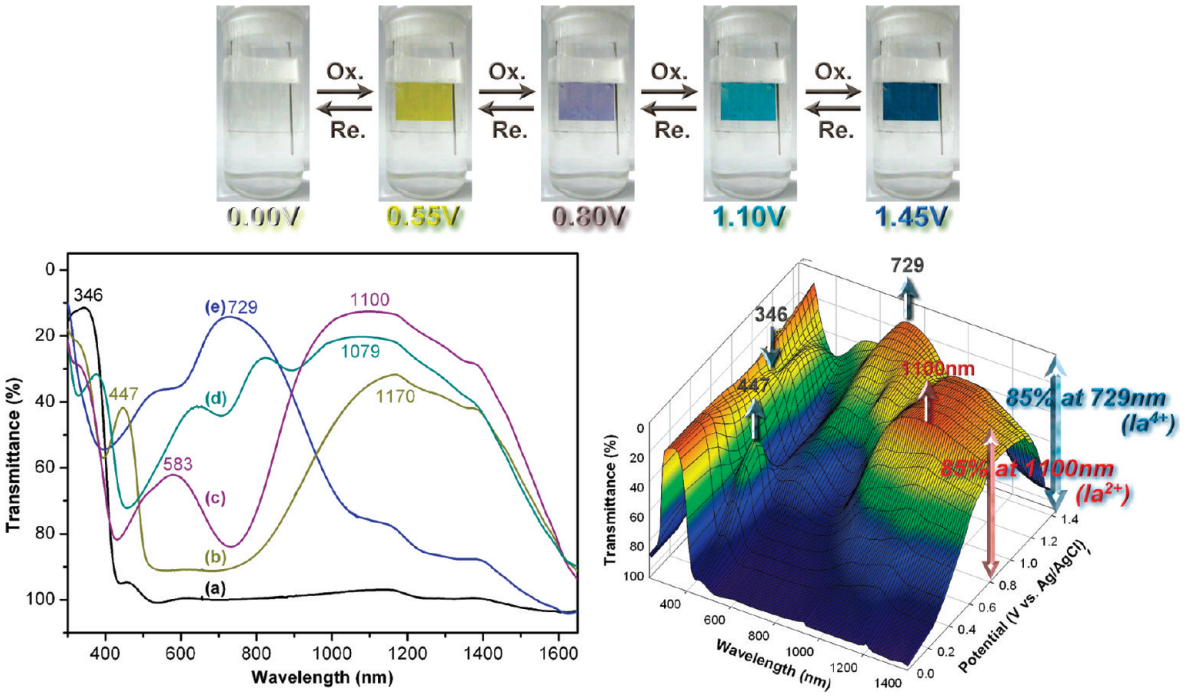

Figure 4. Electrochromic behavior (left) at applied potentials of (a) 0.00, (b) 0.55, (c) 0.80, (d) 1.10, (e) 1.45 (V vs Ag/AgCl), and 3D spectroelectrochemical behavior (right) from 0.00 to 1.45 (V vs Ag/AgCl) of polyamide **Ia** thin film (~120 nm in thickness) on the ITO-coated glass substrate in 0.1 M TBAP/CH_3CN.

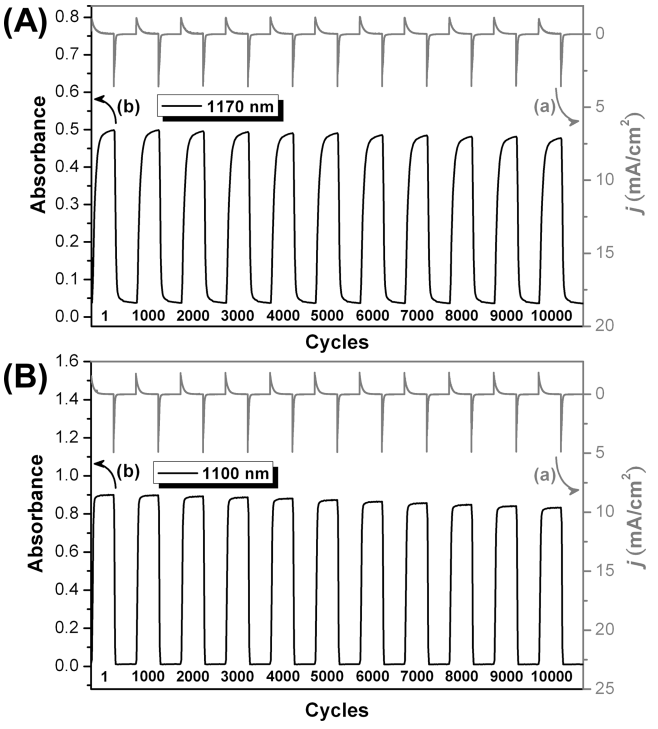

Figure 5. Electrochromic switching between (A) 0 and 0.55 V and (B) 0 and 0.80 V (vs Ag/AgCl) of polyamide **Ia** thin film (~120 nm in thickness) on the ITO-coated glass substrate (coated area: 1.2 cm × 0.5 cm) in 0.1 M TBAP/CH_3CN with a cycle time of 30 s. (a) Current consumption and (b) absorbance change monitored at the given wavelength.

and survive for more than thousands of redox cycles. The polymer **Ia** shows good contrast both in the visible and NIR regions with an extremely high optical transmittance change ($\Delta\%T$) of 85% at 1100 nm for purple coloring at the second oxidation stage, and 85% at 729 nm for blue coloring at the fourth oxidation stage, respectively. Because of the apparent high electrochromic contrast, optical switching studies were investigated more deeply to manifest the outstanding electrochromic characteristics of these obtained novel anodically electrochromic materials.

Electrochromic Switching Studies. For electrochromic switching studies, polymer films were cast on ITO-coated glass slides in the same manner as described above, and chronoamperometric and absorbance measurements were performed. While the films were switched, the absorbance at the given wavelength was monitored as a function of time with UV−vis−NIR spectroscopy. Switching data for the representative cast film of polyamide **Ia** were shown in Figures S9 and S10 in the Supporting Information and Figure 5. The switching time was calculated at 90% of the full switch because it is difficult to perceive any further color change with naked eye beyond this point. As depicted in Figure S9a in the Supporting Information, when the potential was switched between 0 and 0.55 V, polyamide **Ia** thin film revealed switching time of 2.06 s for coloring process and 0.90 s for bleaching. When the switched potential was set between 0 and 0.80 V, thin film **Ia** required 1.82 s for coloration and 1.06 s for bleaching (Figure S9b in the Supporting Information). The polyamides switched quickly between the highly transmissive neutral state and the colored oxidized state. Two movies of electrochromic switches between neutral and oxidation states with a cycle time of 6 s were provided in the Supporting Information. The amount of injected/ejected charge (Q) were calculated by integration of the current density and time obtained from Figure S9c in the Supporting Information as 1.679 and 1.677 mC/cm^2 for oxidation and reduction process at the first oxidation stage, respectively. The ratio of the charge density was 99.9%, indicated that charge injected/ejected was

dx.doi.org/10.1021/cm103552k |*Chem. Mater.* 2011, 23, 1874–1882

Table 2. Optical and Electrochemical Data Collected for Coloration Efficiency Measurements of Polyamide Ia

cycling times[a]	δ%T_{1170}	δOD_{1170}[b]	Q (mC/cm^2)[c]	η (cm^2/C)[d]	decay (%)[e]
1	60	0.487	1.679	290	0
1000	60	0.487	1.679	290	0
2000	60	0.484	1.680	288	0.69
3000	59	0.482	1.678	287	1.03
4000	59	0.479	1.675	286	1.38
5000	59	0.479	1.675	286	1.38
6000	59	0.474	1.674	283	2.41
7000	59	0.473	1.672	283	2.41
8000	58	0.470	1.672	281	3.10
9000	58	0.470	1.671	281	3.10
10000	58	0.466	1.669	279	3.80

[a] Switching between 0.00 and 0.55 (V vs Ag/AgCl). [b] Optical density change at 1170 nm. [c] Ejected charge, determined from the in situ experiments. [d] Coloration efficiency is derived from the equation: $\eta = \delta OD_{1170}/Q$. [e] Decay of coloration efficiency after cyclic scans.

Table 3. Optical and Electrochemical Data Collected for Coloration Efficiency Measurements of Polyamide Ia

cycling times[a]	δ%T_{1100}	δOD_{1100}[b]	Q (mC/cm^2)[c]	η (cm^2/C)[d]	decay (%)[e]
1	85	0.888	2.622	339	0
1000	85	0.886	2.621	338	0.29
2000	85	0.880	2.622	336	0.88
3000	85	0.875	2.621	334	1.47
4000	84	0.869	2.619	332	2.06
5000	84	0.861	2.617	329	2.95
6000	84	0.853	2.615	326	3.83
7000	84	0.845	2.612	324	4.42
8000	84	0.837	2.610	321	5.31
9000	83	0.830	2.607	318	6.19
10000	83	0.822	2.605	316	6.78

[a] Switching between 0.00 and 0.80 (V vs Ag/AgCl). [b] Optical density change at 1100 nm. [c] Ejected charge, determined from the in situ experiments. [d] Coloration efficiency is derived from the equation: $\eta = \delta OD_{1100}/Q$. [e] Decay of coloration efficiency after cyclic scans.

highly reversible during the electrochemical reactions. As shown in Figure S10 in the Supporting Information and Figure 5, the electrochromic stability of the polyamide **Ia** film was determined by measuring the transmittance and optical changes as a function of the number of switching cycles and plotted every 1000th cycle. The electrochromic CE ($\eta = \delta OD/Q$) and injected charge (electroactivity) after various switching steps were monitored and summarized in Tables 2 and 3. The electrochromic film of **Ia** was found to exhibit high CE up to 290 cm^2/C at 1170 nm, and to retain more than 99% of their electroactivity after switching 10,000 times between 0 and 0.55 V (Figure 5A). As the applied switching potential increased to 0.80 V, a higher CE (339 cm^2/C at 1100 nm) could be obtained and showed only 0.7% decay of its electroactivity after 10,000 cycles (Figure 5B). Additional, Figure 6 show the long-term stability measured by keeping 5 h for each coloring process at applied potentials of 0.55 and 0.80 V, respectively, and the relatively high electrochromic stability was observed, which reinforces and affords positive proof of these NIR

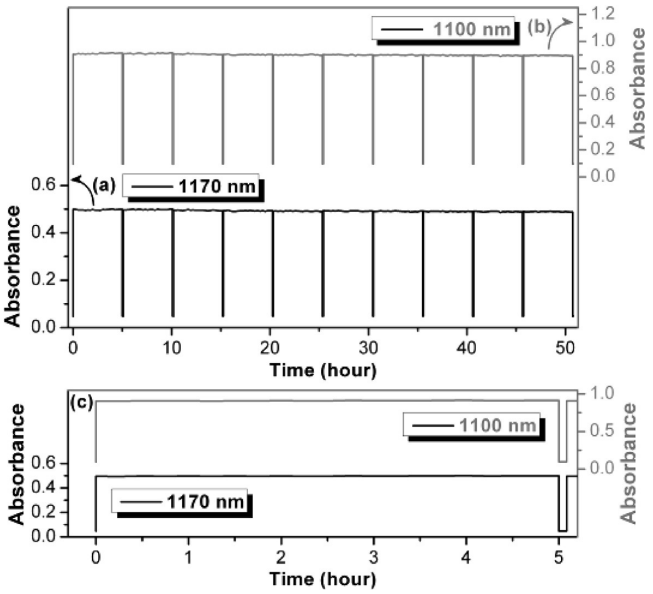

Figure 6. Potential step absorptometry during the continuous cycling test by switching potentials between (a) 0 and 0.55 V, (b) 0 and 0.80 V (vs Ag/AgCl), and (c) absorptometry for 1 switching cycle of polyamide **Ia** thin film (~120 nm in thickness) on the ITO-coated glass substrate (coated area: 1.2 cm × 0.5 cm) in 0.1 M TBAP/CH_3CN with a cycle time of 5 h and 5 min for coloring and bleaching processes, respectively.

electroactive aromatic polyamides with the potential for commercial applications. Considering the retained contrast ratio and electroactive stability during electrochromic operation, these novel polyamides show highly electrochromic stability compared with other electrochromic polymers.[5]

CONCLUSIONS

A series of novel NIR electrochromic aromatic polyamides with starburst triarylamine units were readily prepared from the newly synthesized diamine monomer, *N*,*N*-bis[4-(4-methoxyphenyl-4′-aminophenylamino)phenyl]-*N*′,*N*′-di(4-methoxyphenyl)-*p*-phenylenediamine, with various aromatic dicarboxylic acids via the phosphorylation polyamidation. Introduction of highly electron-donating starburst triarylamine group to the polymer main chain not only stabilizes its radical cations but also leads to good solubility and film-forming properties of the polyamides. In addition to high T_g and good thermal stability, all the obtained polymers also reveal valuable electrochromic characteristics such as high contrast ratio both in the visible range and NIR region, low switching times, high coloration efficiency, and highly electrochromic/electroactive reversibility. Thus, these characteristics suggest that these novel starburst triarylamine-containing electrochromic aromatic polyamides have great potential for practical applications in both visible and NIR region.

EXPERIMENTAL SECTION

Materials. *N*,*N*-Bis(4-bromophenyl)-*N*′,*N*′-di(4-methoxyphenyl)-*p*-phenylenediamine[13] and 4-methoxy-4′-nitrodiphenylamine[12] were synthesized according to a previously reported procedure. Commercially available aromatic dicarboxylic acids such as 4,4′-oxidibenzoic acid (**3a**) and 2,2′-bis(4-carboxyphenyl)hexafluoropropane (**3b**) were purchased from Tokyo Chemical Industry (TCI) Co. and used as received. Commercially obtained anhydrous calcium chloride ($CaCl_2$) was dried under vacuum at 180 °C for 8 h. Tetrabutylammonium perchlorate (TBAP) (Acros) was

recrystallized twice by ethyl acetate in a nitrogen atmosphere and then dried in vacuo prior to use. All other reagents were used as received from commercial sources.

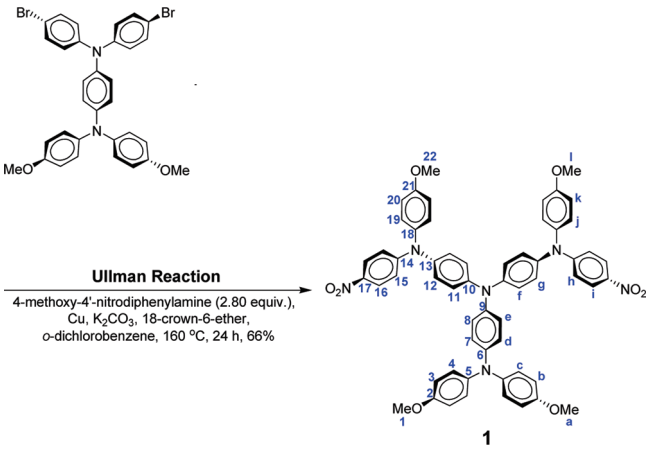

1

*N,N-Bis[4-(4-methoxyphenyl-4′-nitrophenylamino)phenyl]-N′,N′-di(4-methoxyphenyl)-p-phenylenediamine (**1**).* In a 100 mL three-neck round-bottom flask equipped with a stirring bar in a nitrogen atmosphere, 2.80 g (4.41 mmol) of *N,N*-bis(4-bromophenyl)-*N′,N′*-di(4-methoxyphenyl)-*p*-phenylenediamine, 3.02 g (12.35 mmol) of 4-methoxy-4′-nitrodiphenylamine, 4.89 g (35.39 mmol) of powdered anhydrous potassium carbonate, 1.12 g (17.64 mmol) of copper powder, and 0.23 g (0.88 mmol) of 18-crown-6-ether were stirred in 40 mL of *o*-dichlorobenzene at 160 °C for 24 h in a nitrogen atmosphere. The copper and inorganic salts were then removed by filtration of the hot reaction mixture, and the product was precipitated into ethanol. The product was recrystallized by ethyl acetate to give 2.79 g (66% in yield) of dark red solid with a mp of 231−233 °C (measured by DSC at 10 °C/min). FT-IR (KBr pellet, cm^{-1}): 1587, 1311 (-NO_2 stretch), 1243, 1034 (-C-O-C- stretch). ^{1}H NMR (DMSO-d_6, δ, ppm): 3.72 (s, -OCH_3), 3.77 (s, -OCH_3), 6.69 (d, 4H), 6.77(d, 2H), 6.89 (d, 4H), 6.97−7.04 (m, 14H), 7.19 (d, 4H), 7.25 (d, 4H), 8.02 (d, 4H). ^{13}C NMR (DMSO-d_6, δ, ppm): 55.40 (C^1), 55.54 (C^{22}), 115.15, 115.25, 115.72, 120.83, 123.65, 125.86, 126.70, 127.25, 128.00, 129.00, 137.54, 138.22, 138.86, 140.30, 145.40, 145.54, 154.11, 155.86, 157.93. Anal. Calcd for $C_{58}H_{48}N_6O_8$ (957.04): C, 72.79%; H, 5.06%; N, 8.78%. Found: C, 72.19%; H, 5.13%; N, 8.66%. ESI-MS: calcd for $(C_{58}H_{48}N_6O_8)^+$, *m/z* 957.0; found, *m/z* 956.4.

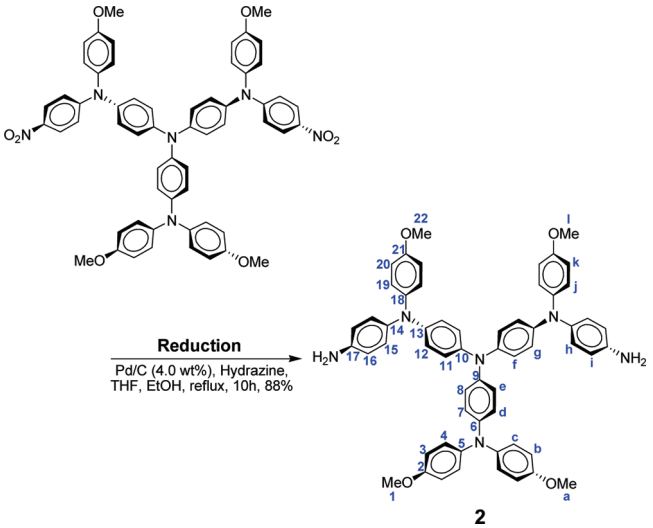

2

*N,N-Bis[4-(4-methoxyphenyl-4′-aminophenylamino)phenyl]-N′,N′-di(4-methoxyphenyl)-p-phenylenediamine (**2**).* In a 100 -mL three-neck round-bottom flask equipped with a stirring bar in a nitrogen atmosphere, 730.9 mg (0.76 mmol) of dinitro compound (**2**) and 29.0 mg of 10% Pd/C were dissolved/suspended in 10 mL of ethanol and 15 mL of THF. The suspension solution was heated to reflux, and 0.4 mL of hydrazine monohydrate was added slowly to the mixture, and the solution was then stirred at reflux temperature for 10 h, the solution was filtered to remove Pd/C. After concentrated the filtrate, the product was washed thoroughly with ethanol and dried in vacuo at 80 °C to afford 603.4 mg (88% in yield) of bright yellow powders with a mp of 254−256 °C (measured by DSC at 10 °C/min) FT-IR (KBr pellet, cm^{-1}): 3446, 3365 (N−H stretch), 1239, 1035 (-C-O-C- stretch). ^{1}H NMR (DMSO-d_6, δ, ppm): 3.68 (s, -OCH_3), 3.69 (s, -OCH_3), 4.98 (s, -NH_2), 6.51 (d, 4H), 6.65 (d, 4H), 6.70−6.80 (m, 12H), 6.83 (d, 8H), 6.91 (d, 8H). ^{13}C NMR (DMSO-d_6, δ, ppm): 55.40 (C^1+C^{22}), 115.00, 115.11, 120.67, 122.65, 123.45, 124.65, 125.05, 125.53, 127.41, 136.13, 140.20, 141.02, 141.29, 141.96, 142.57, 144.10, 145.79, 154.87, 155.20. Anal. Calcd for $C_{58}H_{52}N_6O_4$ (897.07): C, 77.65%; H, 5.84%; N, 9.37%. Found: C, 77.31%; H, 5.75%; N, 9.34%. ESI-MS: calcd for $(C_{58}H_{52}N_6O_4)^+$, *m/z* 897.1; found, *m/z* 896.5.

Polymer Synthesis. The synthesis of polyamide **Ia** was used as an example to illustrate the general synthetic route used to produce the polyamides. A mixture of 577.1 mg (0.64 mmol) of the diamine monomer **2**, 166.1 mg (0.64 mmol) of 4,4′-oxidibenzoic acid (**3a**), 20 mg of calcium chloride, 0.51 mL of triphenyl phosphite, 0.32 mL of pyridine, and 0.51 mL of NMP was heated with stirring at 105 °C for 3 h. The obtained polymer solution was poured slowly into 300 mL of stirred methanol giving rise to a stringy, fiberlike precipitate that was collected by filtration, washed thoroughly with hot water and methanol, and dried under vacuum at 100 °C. Reprecipitations of the polymer by *N,N*-dimethylacetamide (DMAc)/methanol were carried out twice for further purification. The inherent viscosity and weight-average molecular weights (M_w) of the obtained polyamide **Ia** was 0.27 dL/g (measured at a concentration of 0.5 g/dL in DMAc at 30 °C) and 69,800 Da, respectively. The FT-IR spectrum of **Ia** (film) exhibited characteristic amide absorption bands at 3306 cm^{-1} (N−H stretch), 3036 cm^{-1} (aromatic C−H stretch), 2998−2834 cm^{-1} (CH_3 C−H stretch), 1670 cm^{-1} (amide carbonyl), 1240 cm^{-1} (asymmetric stretch C−O−C), 1036 cm^{-1} (symmetric stretch C−O−C). ^{1}H NMR (DMSO-d_6, δ, ppm): 3.70 (s, -OCH_3), 6.74−6.99 (m, 32H), 7.17 (d, 4H), 7.62 (d, 4H), 8.00 (d, 4H), 10.14 (s, 2H, amide-NH). Anal. Calcd (%) of **Ia** for $(C_{74}H_{64}N_6O_7)_n$ (1149.34)$_n$: C, 77.33; H, 5.61; N, 7.31. Found: C, 75.35; H, 5.39; N, 7.13. The other polyamide **Ib** were prepared by an analogous procedure. The FT-IR spectrum of **Ib** (film) exhibited characteristic amide absorption bands at 3307 cm^{-1} (N−H stretch), 3036 cm^{-1} (aromatic C−H stretch), 2998−2834 cm^{-1} (CH_3 C−H stretch), 1669 cm^{-1} (amide carbonyl), 1242 cm^{-1} (asymmetric stretch C−O−C), 1037 cm^{-1} (symmetric stretch C−O−C). ^{1}H NMR (DMSO-d_6, δ, ppm): 3.68 (s, -OCH_3), 6.72−6.96 (m, 32H), 7.48 (d, 4H), 7.61 (d, 4H), 7.99 (d, 4H), 10.31 (s, 2H, amide-NH). Anal. Calcd (%) of **Ib** for $(C_{77}H_{64}F_6N_6O_6)_n$ (1283.36)$_n$: C, 72.06; H, 5.03; N, 6.55. Found: C, 70.80; H, 4.81; N, 6.61.

Preparation of the Polyamide Films. A solution of polymer was made by dissolving about 0.6 g of the polyamide sample in 9 mL of DMAc. The homogeneous solution was poured into a 9-cm glass Petri dish, which was placed in a 90 °C oven for 5 h to remove most of the solvent; then the semidried film was further dried in vacuo at 160 °C for 8 h. The obtained films were about 60 μm in thickness and were used for solubility tests and thermal analyses.

Measurements. Fourier transform infrared (FT-IR) spectra were recorded on a PerkinElmer Spectrum 100 Model FT-IR spectrometer. Elemental analyses were run in a Heraeus VarioEL-III CHNS elemental analyzer. ^{1}H NMR spectra were measured on a Bruker AC-300 MHz

spectrometer in DMSO-d_6, using tetramethylsilane as an internal reference, and peak multiplicity was reported as follows: s, singlet; d, doublet. The inherent viscosities were determined at 0.5 g/dL concentration using Tamson TV-2000 viscometer at 30 °C. Gel permeation chromatographic (GPC) analysis was carried out on a Waters chromatography unit interfaced with a Waters 2410 refractive index detector. Two Waters 5 μm Styragel HR-2 and HR-4 columns (7.8 mm I. D. × 300 mm) were connected in series with NMP as the eluent at a flow rate of 0.5 mL/min at 40 °C and were calibrated with polystyrene standards. Thermogravimetric analysis (TGA) was conducted with a PerkinElmer Pyris 1 TGA. Experiments were carried out on approximately 6−8 mg film samples heated in flowing nitrogen or air (flow rate = 20 cm^3/min) at a heating rate of 20 °C/min. DSC analyses were performed on a PerkinElmer Pyris 1 DSC at a scan rate of 10 °C/min in flowing nitrogen (20 cm^3/min). Electrochemistry was performed with a CH Instruments 611B electrochemical analyzer. Voltammograms are presented with the positive potential pointing to the left and with increasing anodic currents pointing downward. Cyclic voltammetry (CV) was conducted with the use of a three-electrode cell in which ITO (polymer films area about 0.5 cm × 1.2 cm) was used as a working electrode. A platinum wire was used as an auxiliary electrode. All cell potentials were taken by using a homemade Ag/AgCl, KCl (sat.) reference electrode. Spectroelectrochemical experiments were carried out in a cell built from a 1 cm commercial UV−visible cuvette using Hewlett-Packard 8453 UV−visible diode array, Jasco V-570 UV−vis/NIR, and Hitachi U-4100 UV−vis−NIR spectrophotometer. The ITO-coated glass slide was used as the working electrode, a platinum wire as the counter electrode, and an Ag/AgCl cell as the reference electrode. CE (η) determines the amount of optical density change (δOD) at a specific absorption wavelength induced as a function of the injected/ejected charge (Q) which is determined from the in situ experiments. CE is given by the equation: $\eta = \delta OD/Q = \log[T_b/T_c]/Q$, where η (cm^2/C) is the coloration efficiency at a given wavelength, and T_b and T_c are the bleached and colored transmittance values, respectively. The thickness of the polyamide thin films was measured by alpha-step profilometer (Kosaka Lab., Surfcorder ET3000, Japan). Colorimetry measurements were obtained using a Minolta CS-100A Chroma Meter. The color coordinates are expressed in the CIE 1931 Yxy color spaces.

■ ASSOCIATED CONTENT

Supporting Information. Two movies of electrochromic switches between neutral and oxidation states. Table: inherent viscosity, molecular weights, solubility behavior, and thermal properties. Figure: NMR of monomers, IR of monomers and polyamide, TGA, DSC traces and CV of polyamides, calculation of optical switching time of polyamides. This material is available free of charge via the Internet at http://pubs.acs.org.

■ AUTHOR INFORMATION

Corresponding Author
*E-mail: gsliou@ntu.edu.tw.

■ ACKNOWLEDGMENT

The authors are grateful to the National Science Council of the Republic of China for financial support of this work. And also to C.-W. Lu of the Instrumentation Center, National Taiwan University, for CHNS (EA) analysis experiments. C. H. Ho

■ REFERENCES

(1) (a) Monk, P. M. S.; Mortimer, R. J.; Rosseinsky, D. R. *Electrochromism and Electrochromic Devices*; Cambridge University Press: Cambridge, U.K., 2007. (b) Mortimer, R. J. *Chem. Soc. Rev.* **1997**, *26*, 147. (c) Rosseinsky, D. R.; Mortimer, R. J. *Adv. Mater.* **2001**, *13*, 783. (d) Somani, P. R.; Radhakrishnan, S. *Mater. Chem. Phys.* **2003**, *77*, 117. (e) Liu, S.; Kurth, D. G.; Mohwald, H.; Volkmer, D. *Adv. Mater.* **2002**, *14*, 225. (f) Zhang, T.; Liu, S.; Kurth, D. G.; Faul, C. F. J. *Adv. Funct. Mater.* **2009**, *19*, 642. (g) Maier, A.; Rabindranath, A. R.; Tieke, B. *Adv. Mater.* **2009**, *21*, 959. (h) Motiei, L.; Lahav, M.; Freeman, D.; van der Boom, M. E. *J. Am. Chem. Soc.* **2009**, *131*, 3468. (i) Beaujuge, P. M.; Reynolds, J. R. *Chem. Rev.* **2010**, *110*, 268.

(2) (a) Bach, U.; Corr, D.; Lupo, D.; Pichot, F.; Ryan, M. *Adv. Mater.* **2002**, *14*, 845. (b) Dyer, A. L.; Grenier, C. R. G.; Reynolds, J. R. *Adv. Funct. Mater.* **2007**, *17*, 1480. (c) Ma, C.; Taya, M.; Xu, C. *Polym. Eng. Sci.* **2008**, *48*, 2224. (d) Beaupre, S.; Breton, A. C.; Dumas, J.; Leclerc, M. *Chem. Mater.* **2009**, *21*, 1504.

(3) (a) Rose, T. L.; D'Antonio, S.; Jillson, M. H.; Kon, A. B.; Suresh, R.; Wang, F. *Synth. Met.* **1997**, *85*, 1439. (b) Franke, E. B.; Trimble, C. L.; Hale, J. S.; Schubert, M.; Woollam, J. A. *J. Appl. Phys.* **2000**, *88*, 5777. (c) Topart, P.; Hourquebie, P. *Thin Solid Films* **1999**, *352*, 243.

(4) (a) Vickers, S. J.; Ward, M. D. *Electrochem. Commun.* **2005**, *7*, 389. (b) Schwab, P. F. H.; Diegoli, S.; Biancardo, M.; Bignozzi, C. A. *Inorg. Chem.* **2003**, *42*, 6613. (c) Qi, Y.; Wang, Z. Y. *Macromolecules* **2003**, *36*, 3146. (d) Wang, S.; Todd, E. K.; Birau, M.; Zhang, J.; Wan, X.; Wang, Z. Y. *Chem. Mater.* **2005**, *17*, 6388. (e) Qiao, W.; Zheng, J.; Wang, Y.; Zheng, Y.; Song, N.; Wan, X.; Wang, Z. Y. *Org. Lett.* **2008**, *10*, 641. (f) Zheng, J.; Qiao, W.; Wan, X.; Gao, J. P.; Wang, Z. Y. *Chem. Mater.* **2008**, *20*, 6163. (g) Hasanain, F.; Wang, Z. Y. *Dyes, Pigments* **2009**, *83*, 95.

(5) (a) Shi, P.; Amb, C. M.; Knott, E. P.; Thompson, E. J.; Liu, D. Y.; Mei, J.; Dyer, A. L.; Reynolds, J. R. *Adv. Mater.* **2010**, *22*, 4949. (b) Sonmez, G.; Meng, H.; Zhang, Q.; Wudl, F. *Adv. Funct. Mater.* **2003**, *13*, 726. (c) Sonmez, G.; Meng, H.; Wudl, F. *Chem. Mater.* **2004**, *16*, 574. (d) Li, M.; Patra, A.; Sheynin, Y.; Bendikov, M. *Adv. Mater.* **2009**, *21*, 1707. (e) Aubert, P. H.; Argun, A. A.; Cirpan, A.; Tanner, D. B.; Reynolds, J. R. *Chem. Mater.* **2004**, *16*, 2386.

(6) (a) Creutz, C.; Taube, H. *J. Am. Chem. Soc.* **1973**, *95*, 1086. (b) Lambert, C.; Noll, G. *J. Am. Chem. Soc.* **1999**, *121*, 8434.

(7) Robin, M.; Day, P. *Adv. Inorg. Radiochem.* **1967**, *10*, 247.

(8) Szeghalmi, A. V.; Erdmann, M.; Engel, V.; Schmitt, M.; Amthor, S.; Kriegisch, V.; Noll, G.; Stahl, R.; Lambert, C.; Leusser, D.; Stalke, D.; Zabel, M.; Popp, J. *J. Am. Chem. Soc.* **2004**, *126*, 7834.

(9) (a) Cheng, S. H.; Hsiao, S. H.; Su, T. X.; Liou, G. S. *Macromolecules* **2005**, *38*, 307. (b) Liou, G. S.; Hsiao, S. H.; Su, T. X. *J. Mater. Chem.* **2005**, *15*, 1812. (c) Liou, G. S.; Yang, Y. L.; Su, Y. L. O. *J. Polym. Sci., Part A: Polym. Chem.* **2006**, *44*, 2587. (d) Liou, G. S.; Hsiao, S. H.; Chen, H. W. *J. Mater. Chem.* **2006**, *16*, 1831. (e) Liou, G. S.; Hsiao, S. H.; Huang, N. K.; Yang, Y. L. *Macromolecules* **2006**, *39*, 5337. (f) Liou, G. S.; Chen, H. W.; Yen, H. J. *J. Polym. Sci., Part A: Polym. Chem.* **2006**, *44*, 4108. (g) Liou, G. S.; Chen, H. W.; Yen, H. J. *Macromol. Chem. Phys.* **2006**, *207*, 1589. (h) Liou, G. S.; Chang, C. W.; Huang, H. M.; Hsiao, S. H. *J. Polym. Sci., Part A: Polym. Chem.* **2007**, *45*, 2004. (i) Liou, G. S.; Hsiao, S. H.; Chen, W. C.; Yen, H. J. *Macromolecules* **2006**, *39*, 6036. (j) Liou, G. S.; Yen, H. J. *J. Polym. Sci., Part A: Polym. Chem.* **2006**, *44*, 6094. (k) Yen, H. J.; Liou, G. S. *J. Polym. Sci., Part A: Polym. Chem.* **2009**, *47*, 1584. (l) Yen, H. J.; Liou, G. S. *J. Mater. Chem.* **2010**, *20*, 9886.

(10) (a) Chang, C. W.; Liou, G. S.; Hsiao, S. H. *J. Mater. Chem.* **2007**, *17*, 1007. (b) Liou, G. S.; Chang, C. W. *Macromolecules* **2008**, *41*, 1667. (c) Hsiao, S. H.; Liou, G. S.; Kung, Y. C.; Yen, H. J. *Macromolecules* **2008**, *41*, 2800. (d) Chang, C. W.; Chung, C. H.; Liou, G. S. *Macromolecules* **2008**, *41*, 8441. (e) Chang, C. W.; Liou, G. S. *J. Mater. Chem.* **2008**, *18*, 5638. (f) Chang, C. W.; Yen, H. J.; Huang, K. Y.; Yeh, J. M.; Liou, G. S. *J. Polym. Sci., Part A: Polym. Chem.* **2008**, *46*, 7937. (g) Yen, H. J.; Liou, G. S. *Chem. Mater.* **2009**, *21*, 4062. (h) Yen, H. J.; Liou, G. S. *Org. Electron* **2010**, *11*, 299. (i) Huang, L. T.; Yen, H. J.; Chang, C. W.; Liou, G. S. *J. Polym. Sci., Part A: Polym. Chem.* **2010**, *48*, 4747.

(11) Yamazaki, N.; Matsumoto, M.; Higashi, F. *J. Polym. Sci. Polym. Chem. Ed.* **1975**, *13*, 1373.

(12) Liou, G. S.; Lin, H. Y. *Macromolecules* **2009**, *42*, 125.

(13) Chang, H. W.; Lin, K. H.; Chueh, C. C.; Liou, G. S.; Chen, W. C. *J. Polym. Sci., Part A: Polym. Chem.* **2009**, *47*, 4037.